Phys. Status Solidi RRL **7**, No. 11, 955–958 (2013) / **DOI** 10.1002/pssr.201308090

Wafer thickness optimization for silicon solar cells of heterogeneous material quality

Bernhard Michl [*, 1], **Martin Kasemann** [2], **Wilhelm Warta** [1], **and Martin C. Schubert** [1]

[1] Fraunhofer Institut für Solare Energiesysteme, Heidenhofstr. 2, 79110 Freiburg, Germany
[2] Department of Microsystems Engineering, Albert-Ludwig University of Freiburg, 79110 Freiburg, Germany

Received 22 July 2013, revised 7 August 2013, accepted 8 August 2013
Published online 13 August 2013

Keywords wafer thickness, multicrystalline, silicon, solar cell

[*] Corresponding author: e-mail bernhard.michl@ise.fraunhofer.de, Phone: +49 761 4588 5201, Fax: +49 761 4588 9250

In this Letter, we introduce a method of calculating the optimal wafer thickness for silicon solar cells with multicrystalline bulk material. The optimal thickness depends on the relation of bulk recombination to surface recombination and the light trapping. For multicrystalline silicon bulk recombination strongly varies laterally and with injection level, which complicates the calculations. A thickness optimization using the "Efficiency Limiting Bulk Recombination Analysis" (ELBA) takes all these effects correctly into account.

1 Introduction With the development of wafering technologies for thin wafers, there is a trend towards high-efficiency solar cells on thin substrates [1, 2], especially for monocrystalline high-efficiency cells [3]. However, concerning multicrystalline material there are few investigations in literature on the influence of wafer thickness on mc-Si solar cell performance [4–6]. These studies on solar cells are challenging as neighbouring wafers with comparable electrical quality but differing wafer thicknesses have to be used. After an ordinary sawing process all neighbouring wafers are equally thick. For the standard acidic texturing the saw damage is needed [7], so a special sawing process to obtain sister wafers with different thicknesses is the only solution [4, 5]. Using advanced texturing methods (like the honeycomb texture), mechanically grinding for thinning the wafers is also applicable [6]. With this method, the current mc-Si world record of 20.3% efficiency was achieved with a 99 µm thin wafer. For a thicker wafer (218 µm) the efficiency was 19.9% [6]. Besides the challenges in wafer preparation, the manufacturing of cells is further complicated as the solar cell process has to be adapted for every wafer thickness. For example non-optimal firing conditions can lead to significant scattering in the fill factor [4].

In this paper, we therefore propose an "Efficiency limiting bulk recombination analysis" (ELBA) [8] to calculate the optimum thickness. The approach is based on surface passivated lifetime samples having received the relevant high-temperature steps. A spatially resolved and injection-dependent measurement of the bulk recombination is combined with the information about cell injection conditions obtained from cell simulations. The thickness variation is included in the cell models; the thickness of the lifetime sample is irrelevant. The advantage is that the input data is not related to the solar cell structure itself, so different cell models can be investigated easily. Furthermore, there is no process induced scattering of the data and low cell thicknesses can be investigated without yield problems.

2 Approach

2.1 ELBA For the analysis we use the ELBA approach; details can be found in [8]. So a spatially resolved injection-dependent bulk lifetime measurement is combined with a PC1D simulation to calculate the local and global cell efficiency. There are some modifications to the approach in [8]: (i) Maximum power point (MPP) injection conditions were not simulated by a simulated Suns-V_{oc} curve, but a PC1D *IV*-curve, which better reflects the injection conditions in the cell. (ii) For averaging the spatially re-

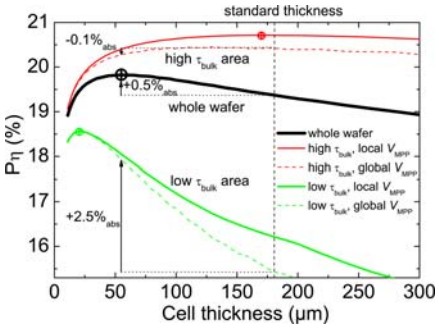

Figure 1 Dependence of global and local pseudo efficiency (at the local and global MPP) in the PERC process on cell thickness of material 1. The dots indicate the position of the maximum efficiency. The arrows denote efficiency gains/losses of a cell at the global optimum thickness of 55 µm compared to the standard thickness of 180 µm. The positions of the two regions are marked in Fig. 2.

solved results of short-circuit current density J_{sc}, open-circuit voltage V_{oc} and efficiency η we use the method of Isenberg *et al.* [9]. The weighing functions $J(V_{sc/MPP/oc}, \tau_{bulk})$ for averaging the lifetime images $\tau_{xy,sc/MPP/oc}$ are directly taken from the PC1D model. (iii) At MPP conditions lateral voltage balancing between regions of different bulk recombination leads to a homogeneous applied global voltage $V_{MPP,global}$ at the entire cell independent of the local lifetime (only R_s leads to local differences, which is neglected here). This was confirmed by Spice network simulations on a mc-Si symmetry element. This effect of voltage balancing is accounted for in ELBA as it not only calculates the local efficiency at the local MPP, but also the local efficiency at the global $V_{MPP,global}$. $V_{MPP,global}$ is calculated from the averaged lifetime $\tau_{bulk,MPP,average}$. The globally applied $V_{MPP,global}$ changes the injection conditions (and therefore bulk lifetimes) and power output compared to the case of the local optimum MPP (so $V_{MPP,global}(\tau_{bulk,MPP,average})$ has to be iteratively improved).

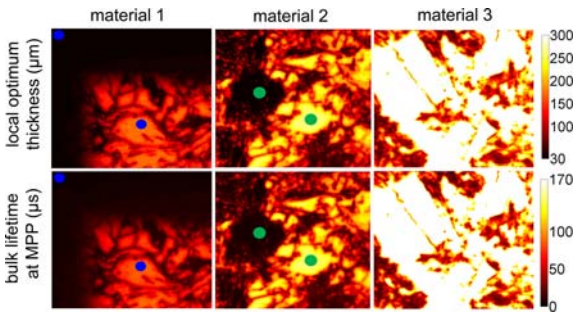

Figure 2 Upper images: Optimum local thickness (calculated at local MPP) of the three materials in the PERC process. Lower images: Bulk lifetime at global $V_{MPP,global}$ of a 180 µm thick PERC cell (averaged values of whole wafer: material 1: 17 µs, material 2: 26 µs, material 3: 79 µs). In order to concisely show details, only the upper left part of the wafers is presented. The green circles indicate the position of the regions used in Fig. 3. The blue circles show the position of the regions used in Fig. 1.

The averaged efficiency of the whole cell is calculated via $V_{MPP,global}(\tau_{bulk,MPP,average}) \cdot J(V_{MPP,global}, \tau_{bulk,MPP,average})$. This procedure takes lateral voltage balancing at the MPP into account, so Spice network simulations are not necessarily needed for the MPP image and, therefore, were not performed in this study. In Fig. 1 the power loss because of the globally applied V_{MPP} is shown for two exemplary regions.

ELBA is ideally suited for wafer thickness optimization for the following reasons: (i) It accounts for the local injection-dependent bulk lifetime and uses the correct injection level at the corresponding operating conditions and wafer thickness based on a cell simulation. (ii) It exploits the spatially resolved lifetime information and averages the images to obtain values for the whole wafer. (iii) The light trapping model needed to correctly describe the light absorption for different wafer thicknesses is included in the PC1D cell model.

2.2 Material and cell properties In this investigation we use three different mc-Si wafers with different material quality (material 1: low quality with a region of impurity in-diffusion from the crystallization crucible, base resistivity 1.1 Ω cm; material 2: medium quality, 1.4 Ω cm; material 3: high quality, 1.5 Ω cm; see Fig. 2 for the bulk lifetime at MPP). The p-type wafers have gone through typical high-temperature steps of a cell process. Subsequently, all layers and the emitter are etched away and the samples are surface passivated with ALD Al_2O_3. Each of the three materials is investigated in three different cell models: (1) An aluminium back-surface-field (Al-BSF) process with isotextured front side yielding a maximum efficiency of 18.5% for a 200 µm 1.0 Ω cm cell with negligible bulk recombination (FZ material) and negligible series resistance R_s losses. The optical model of PC1D is used [10]; external front reflectance (linearly extrapolated into the infrared) and infrared light escaping after penetrating into the cell (for the internal reflectances) are adjusted to the measured reflectivity of the isotextured cells in [8]. (2) A cell structure with dielectric rear side passivation (PERC) and a honeycomb optics on the front side (η = 21.4% for a 200 µm 1.0 Ω cm FZ-cell without R_s losses). The external front and internal reflectances are adjusted to the measured reflection of the honeycomb-textured cells in [11]. (3) A back-junction (BJ) cell with the phosphorous emitter on the back side, honeycomb texture and the same efficiency potential at a wafer thickness of 200 µm as the PERC front-junction cell. In the following, for better readability, we use the term "efficiency" for the pseudo efficiency without series resistance losses.

3 Results and discussion

3.1 Cell injection conditions with varying wafer thickness It is important to discuss the cell injection conditions of the three models as they reveal at which injection point the bulk lifetime of the mc-Si wafer is evaluated. Figure 3 gives the injection-dependent bulk lifetime of

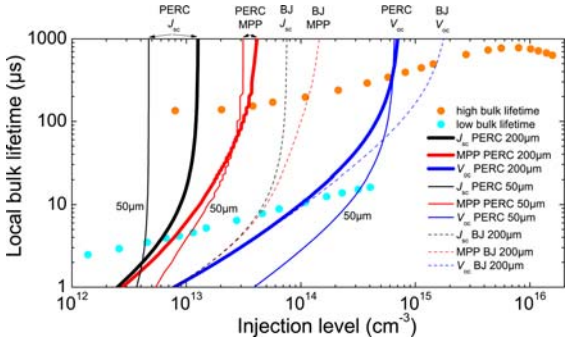

Figure 3 Experimental data of the measured local bulk lifetime of two exemplary regions of material 2 (see Fig. 2; symbols) and the injection conditions of the PERC (thick lines) and BJ (dashed lines) model at J_{sc}, MPP, V_{oc} for a 200 µm thick 1.4 Ω cm cell. For the PERC cell also the case of 50 µm thickness is presented (thin lines). Data of the Al-BSF model is not given for the sake of clarity; the injection levels are below the PERC model.

two exemplary regions on the wafer of material 2 and the injection conditions at open-circuit, MPP and short-circuit for the PERC and BJ cell models for a cell thickness of 200 µm. The intersection between the measured local bulk lifetime and the cell model curve reveals the bulk recombination that is present in the solar cell at the respective operating condition. The injection conditions vary over orders of magnitude from short-circuit (black lines) to MPP (red) and open-circuit (blue) conditions. Most notably, the injection conditions of the back-junction cell are much higher at J_{sc}/MPP conditions due to the reduced charge carrier collection probability at the rear side of the cell.

It is interesting to take a closer look at the changes in injection level when lowering the PERC cell thickness from 200 µm to 50 µm (the qualitative behaviour is the same for the other two cell models). At J_{sc} for most bulk lifetimes the injection level is significantly lower for the 50 µm cell as the charge carriers are collected from the thinner bulk more efficiently. Only for very small bulk lifetimes where the J_{sc} decreases drastically in the thicker cell, the injection level is slightly higher in the thin cell compared to the 200 µm cell. For the high bulk lifetime region the data has to be extrapolated to obtain a value for J_{sc}. As the short-circuit injection level is already in the low level injection plateau of the Shockley–Read–Hall-like curve this is physically justified.

In contrast, at V_{oc} the injection change is totally different: Here for most lifetimes (when the well passivated surfaces are less recombination active than the bulk) the injection level is higher for the thin cell as a result of a higher V_{oc}. As a consequence the injection range from J_{sc} to V_{oc} increases and covers more than two orders of magnitude for the 50 µm cell.

Values at MPP represent an intermediate case: The injection level in the thin cell is higher for low bulk lifetimes; the dominant effect is the efficiency improvement and higher V_{MPP}. For high bulk lifetimes the injection level is lower in the thin cell; here the increased collection probability in a thin cell dominates. These results demonstrate the importance of correctly accounting for the injection dependence of bulk recombination in a thickness analysis.

3.2 Injection-dependent efficiency gain in thinner cells In Figure 3 it is visible that the injection change when lowering the cell thickness leads to a gain or loss in efficiency that is caused by the injection dependence of bulk recombination. The operating conditions of the investigated cell structures are always located in the injection regime with a Shockley–Read–Hall-like increase of lifetime with increasing injection level. Therefore, the shift in MPP injection conditions when lowering the cell thickness leads to a bulk lifetime gain in low lifetime regions and a bulk lifetime loss in high lifetime regions. For the efficiency of the whole wafer the low lifetime regions play the essential role as the performance of high lifetime regions is mostly limited by the cell process. For example, the low lifetime region of material 1 gains 2.5%$_{abs}$ in efficiency in the PERC process when lowering the cell thickness from 180 µm (standard today [1]) to the global optimum value of 55 µm (see Fig. 1). One can divide this gain into different mechanisms: The increased bulk lifetime alone – leaving all other parameters constant – leads to an efficiency gain of 1.0%$_{abs}$. Lowering the cell thickness increases the efficiency by 1.5%$_{abs}$ (including the effect of an increase in $V_{MPP,global}$). This demonstrates the importance of using the local injection-dependent bulk recombination as input information for the thickness optimization procedure.

3.3 Local optimum thickness Images of the local optimum thickness are very instructive as they directly reveal the impact of the inhomogeneous distribution of material properties on the thickness optimization. Figure 2 (upper images) presents images of the local optimum thickness of the three materials in the PERC process. A very broad range from 20 µm to 500 µm optimal thickness is covered according to the broad range in bulk lifetime at MPP (lower images in Fig. 2). The edge region close to the crystallization crucible of material 1 and the dislocation clusters and grain boundaries in all three materials gain in efficiency when using thinner wafers of 100 µm and below. The high lifetime regions would profit from using thicker wafers. The detailed thickness dependence of the efficiency potential in the PERC process of a high lifetime region and a low lifetime region of material 1 is presented in Fig. 1. The curve of the high lifetime region exhibits a rather flat maximum at 170 µm. In contrast, the dislocated region shows a quite sharp maximum at 20 µm. This is the reason why low lifetime regions have a stronger impact on the thickness optimum of the whole wafer (here 55 µm) compared to high lifetime regions. One important factor for the optimum thickness is therefore the ratio of low lifetime regions to high lifetime regions.

3.4 Global optimum thickness For a cell manufacturer the black curve of Fig. 1 is the most important output

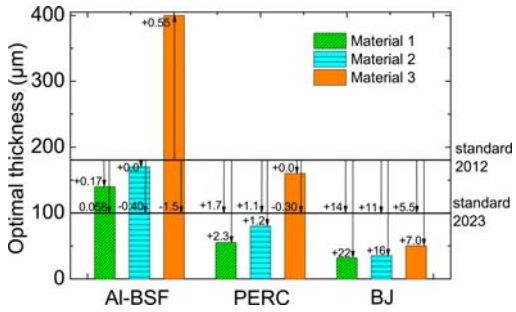

Figure 4 Global optimum thickness of the three materials in the three cell concepts. The numbers at the arrows denote the relative efficiency gain of the optimal thick cell compared to a 180 µm cell in $\%_{rel}$ and the relative gain (+)/loss (–) of a 100 µm cell compared to a 180 µm cell in $\%_{rel}$.

of the optimization procedure. It directly reveals the efficiency gain or loss when altering the cell thickness. This curve in combination with the information of production yield and wafer costs vs. cell thickness can be used to judge if there are potential benefits in altering the currently used wafer thickness. An overview of the thickness optimization results of all three materials and cell processes is given in Fig. 4.

3.4.1 Al-BSF cell For the very good material 3 in the Al-BSF process, it shows that the optimum thickness of 400 µm lies above typical wafer thicknesses nowadays of about 180 µm [1]. Material 1 and 2 perform best with lower thicknesses of about 150 µm. The acidic texture in combination with the low back side reflectance of the Al-BSF is the reason why it is not beneficial to have a lower wafer thickness even for material 1: the short-circuit current decreases dramatically because of the non-ideal light trapping properties of that structure. The efficiency gains of the optimum thickness vs. the standard 180 µm are moderate. However, the good material 3 shows that quite high losses can occur when producing cells with only 100 µm thickness, which is expected to be the standard in 10 years [1].

3.4.2 Back-junction cell Concerning the BJ cell the optimum thickness of all three materials are quite close together at low values of only 32 µm to 50 µm. In a thin wafer it is easier to collect the minority charge carriers on the rear side. The optimum thickness is mostly determined by the light trapping scheme and the material quality has only a minor impact. The efficiency vs. thickness dependence closely follows the short-circuit current vs. thickness dependence. However, even for a 100 µm cell there are high gains in efficiency compared to a 180 µm cell and the gains are strongly dependent on material quality. For example, material 3 exceeds 20% efficiency for a thickness below 130 µm.

3.4.3 PERC cell For the PERC process with honeycomb optics the optimum thicknesses of the three materials are very different ranging from 55 µm to 160 µm. Differences from the material quality are most pronounced in this cell process. The reason is on the one hand that the optical properties (good light trapping) of that structure allow decreasing the cell thickness without having too much absorption loss in J_{sc}. On the other hand, the very good electrical properties (low surface recombination) lead to significant improvements in V_{oc} when using thinner wafers. For material 1 and 2 considerable efficiency gains can be expected for wafers thinner than 180 µm. In contrast, the efficiency of material 3 will suffer in a 100 µm cell compared to 180 µm thickness.

Neglecting the bulk injection dependence can lead to very misleading results. For example, using only the mean ($\tau^{-1/2}$) 1 sun bulk lifetime of a calibrated PL image, the optimum thickness for material 1 in the PERC process would be calculated to be 135 µm, in contrast to 55 µm from ELBA. Adjusting the generation rate can lead to better thickness estimates, but are only useful for a specific material quality.

4 Conclusions The wafer thickness optimization procedure based on ELBA presented in this paper clearly demonstrates the importance of using the information of spatially resolved injection-dependent bulk recombination as input. MPP injection conditions change when changing the cell thickness dependent on the local bulk lifetime. This can lead to additional efficiency gains in low lifetime regions because of lower bulk recombination at the higher injection conditions of a thin cell. The optimum thickness of a wafer is strongly dependent on the investigated cell concept and the material quality. The main factors are the local injection-dependent bulk recombination, the light trapping scheme and surface passivation of the cell structure and the position of the charge carrier collecting junction. Lowering the current standard wafer thickness from 180 µm to 100 µm in a PERC process leads to considerable gains for the materials with higher bulk recombination, but losses were observed for the high quality material.

Acknowledgements The work was supported by the collaborative project "20plµs" funded by the European Commission under FP7 with the contract number 256695. The authors would like to thank REC cells for providing material 3 for this study.

References

[1] International Technology Roadmap for Photovoltaic (ITRPV) Results 2012, March 2013.
[2] B. Terheiden et al., in: Proc. 27th EUPVSEC, Frankfurt, Germany, 2012, pp. 1586–1590.
[3] S. Tohoda et al., J. Non-Cryst. Solids **358**, 2219 (2012).
[4] C. J. J. Tool et al., Prog. Photovolt.: Res. Appl. **10**, 279 (2002).
[5] C. J. J. Tool et al., Sol. Energy Mater. Sol. Cells **90**, 3165 (2006).
[6] O. Schultz et al., Prog. Photovolt.: Res. Appl. **12**, 553 (2004).
[7] R. Einhaus et al., in: Proc. 26th IEEE PVSC, Anaheim, CA, USA, 1997, pp. 167–170.
[8] B. Michl et al., Sol. Energy Mater. Sol. Cells **98**, 441 (2012).
[9] J. Isenberg et al., J. Appl. Phys. **94**, 4122 (2003).
[10] D. A. Clugston et al., in: Proc. 26th IEEE PVSC, Anaheim, CA, USA, 1997, pp. 207–210.
[11] H. Hauser et al., IEEE J. Photovoltaics **2**, 114 (2012).

